

Antimicrobial and nuclease activity of mixed polypyridyl ruthenium(II) complexes

Mohan N. Patel^{a,*}, Pradhuman A. Parmar^a, Deepen S. Gandhi^a, Vasudev R. Thakkar^b

^a Department of Chemistry, Sardar Patel University, Vallabh Vidyanagar-388 120, Gujarat, India

^b BRD School of Bioscience, Sardar Patel University, Vallabh Vidyanagar-388 120, Gujarat, India

ARTICLE INFO

Article history:

Received 8 May 2010

Accepted 17 August 2010

Available online 24 August 2010

Keywords:

Terpyridine

Polypyridyl ruthenium complexes

Partial intercalation

Salt dependence

Thermal denaturation

pUC19 DNA

ABSTRACT

The ruthenium(II) complexes with 2,9-dimethyl-1,10-phenanthroline (dmphen) and terpyridine derivatives have been synthesized and screened for their antimicrobial potency. The interaction of these complexes with Herring Sperm DNA was investigated by thermal denaturation, viscosity measurements, gel electrophoresis and spectrophotometric methods. The results indicate that the complexes bound to DNA via partial intercalative mode. The salt-dependent binding of these complexes has been determined by UV–Vis spectrophotometric titration. The contribution of the non-electrostatic binding free energy (ΔG_t^0) to the total binding free energy change (ΔG^0) is found to be ~88% at $[Na^+] = 0.075$ M. The large value suggests that the stabilization of the DNA binding is mostly due to the contribution of non-electrostatic process.

© 2010 Elsevier B.V. All rights reserved.

The interaction of ruthenium(II) polypyridyl complexes with DNA has been a topic of major bioinorganic interest. Ruthenium polypyridyl complexes have received special attention due to their strong metal to ligand charge transfer (MLCT) absorption, their unique emission characteristics, the perturbation of which could be exploited to study their DNA binding properties [1]. An understanding of how these small molecules bind to DNA will be potentially useful in the design of new drugs, diagnostic reagents, highly sensitive spectroscopic and reactive probes [2,3]. Polypyridyl ruthenium(II) complexes can bind to DNA by non-covalent interactions such as electrostatic binding, groove binding [4], intercalative binding and partial intercalative binding [5,6]. The ancillary ligands can also play an important role in governing DNA binding of the complexes in octahedral polypyridyl Ru^{II} complexes. So it is significant and interesting to find the effects of ancillary ligands on the interaction and binding mode of the complexes to DNA. The strong absorbance caused by metal to ligand charge transfer (MLCT), the spectroscopic characteristics and their perturbations upon binding to DNA of the Ru^{II} complexes provide practicable means to explore their DNA binding mechanisms [7].

Herein, we report the synthesis and characterization of four [Ru^{II}(2^{'''}-pytpy)(dmphen)Cl](ClO₄), [Ru^{II}(3^{'''}-pytpy)(dmphen)Cl](ClO₄), [Ru^{II}(3-boptpy)(dmphen)Cl](ClO₄) and [Ru^{II}(4-boptpy)(dmphen)Cl](ClO₄) complexes {where 2^{'''}-pytpy = 4'-(2^{'''}-pyridyl)-2,2':6',2''-terpyridine, 3^{'''}-pytpy = 4'-(3^{'''}-pyridyl)-2,2':6',2''-terpyridine, 3-boptpy = 4'-(3-benzyloxyphenyl)-2,2':6',2''-terpyridine, 4-boptpy = 4'-(4-benzyloxy-

phenyl)-2,2':6',2''-terpyridine}. All the complexes have been screened for their in-vitro antibacterial activity. The interaction of the complexes with DNA has been investigated by spectroscopic, viscosity measurements, thermal denaturation and gel electrophoresis technique. The salt-dependent binding of the complexes has been also studied using spectrophotometric titration at various concentrations of salt (NaCl).

Terpyridines were synthesized by adding 2-acetylpyridine (2.42 g, 20.0 mmol) to 70 mL ethanolic solution of an aldehyde (10 mmol). KOH pellets (1.4 g, 26 mmol) and aqueous NH₃ (30 mL, 25%, 0.425 mol) were added to the solution and stirred at room temperature for 8 h. An off-white solid formed which was collected by filtration and washed with H₂O (3 × 10 mL) and EtOH (2 × 5 mL). Crystallization from CHCl₃–MeOH gave white crystalline solid.

[Ru^{II}(2^{'''}-pytpy)(dmphen)Cl](ClO₄) (**1**) was synthesized by taking [Ru^{II}(2^{'''}-pytpy)Cl₃] (202 mg, 0.39 mmol), 2,9-dimethyl-1,10-phenanthroline (93 mg, 0.45 mmol), excess LiCl (108 mg, 2.6 mmol) and NEt₃ (0.8 mL) in 40 mL of ethanol and the mixture was refluxed for 2 h under a dinitrogen atmosphere. The initial dark brown color of the solution gradually changed to a deep purple. The solvent was then removed under reduced pressure. The dry mass was dissolved in a minimum volume of acetonitrile, and an excess saturated aqueous solution of NaClO₄ was added to it. The precipitate was filtered off and washed with cold ethanol followed by ice-cold water. The product was dried in vacuum and purified using a silica column. The complex was eluted by 2:1 CH₂Cl₂/CH₃CN. Other complexes were synthesized by the same procedure described above by using different terpyridines.

TGA data of the complexes show no weight loss occurring in the range 80–180 °C. So, there is an absence of coordinated or lattice

* Corresponding author. Tel.: +91 2692 226856x220.

E-mail address: jeenen@gmail.com (M.N. Patel).

water molecule. Both the ligands decompose in one step in the temperature range 360–600 °C. Magnetic moment value of all complexes was found to be zero, which suggests low-spin configuration with d^2sp^3 hybridization for octahedral Ru^{II} complexes.

Perchlorate as a counterion is confirmed by a very strong, broad peak at around 1086 cm^{-1} and the strong, sharp peak at around 625 cm^{-1} [8]. In the spectra of complexes **3** and **4**, band at $\sim 1230\text{ cm}^{-1}$ can be attributed to the asymmetric stretching of aromatic ether. A weak, broad peak at around 3070 cm^{-1} , characteristic of aromatic C–H stretching as well as a sharp peak at around 2930 cm^{-1} , characteristic of C–H stretching of methyl. A sharp peak of medium intensity at around 1600 and 1498 cm^{-1} , characteristic of aromatic ring stretching. An intense, sharp peak at around 760 cm^{-1} , characteristic of C–H out-of-plane deformations, appears as expected from a structure including aromatic rings. A weak, sharp band in the range $490\text{--}520\text{ cm}^{-1}$, characteristic of Ru–N stretching mode. A Ru–Cl stretching mode would be expected in the region less than 400 cm^{-1} [9]. The suggested structure of complex **1** is shown in Fig. 1.

The electronic spectra of the ruthenium complexes were recorded in dimethylsulfoxide medium and the band maxima and molar extinction coefficients are listed in Table 1. The UV–Vis spectrum of Ru^{II} complexes exhibits a typical metal to ligand charge transfer (MLCT) transition due to $Ru(d\pi) \rightarrow \text{terpy}(\pi^*)$ with λ_{max} from 491 to 497 nm ($\epsilon = 18\,670\text{--}22\,210\text{ dm}^3\text{ mol}^{-1}\text{ cm}^{-1}$). The spin allowed metal to ligand charge transfer (MLCT) band in the visible spectral region undergoes an increase in intensity and a red shift, regardless of the electron-donor or electron-acceptor nature of the substituent. Complexes show two bands at around 283 nm ($\epsilon = 45\,714\text{--}57\,283\text{ dm}^3\text{ mol}^{-1}\text{ cm}^{-1}$) and 312 nm ($\epsilon = 42\,356\text{--}56\,132\text{ dm}^3\text{ mol}^{-1}\text{ cm}^{-1}$) due to the overlap of ligand centered transitions $\text{dmphen}(\pi) \rightarrow \text{dmphen}(\pi^*)$ and $\text{terpy}(\pi) \rightarrow \text{terpy}(\pi^*)$ [10].

FAB-mass spectra of all complexes were obtained using *m*-nitro benzyl alcohol as matrix. Peaks at 136, 137, 154, 289 and 307 *m/z* values are due to usage of matrix. For complex **1**, the peak at 793 *m/z* value is assigned as a molecular ion peak associated with matrix (136) and two H^+ ions without perchlorate ion [11]. The base peak observed at *m/z* = 209 is due to the dmphen ligand associated with one proton. Several other fragments at *m/z* 758, 448, 413 and 310 values are observed, attributed to fragments associated with matrix or H^+ ions. The isotopic pattern for ruthenium and chlorine atoms is observed in the spectrum.

All the ligands and their ruthenium complexes were screened in-vitro for their growth inhibitory activity against two Gram^(+ve), *Staphylococcus aureus* and *Bacillus subtilis*, and three Gram^(-ve), *Serratia marcescens*, *Pseudomonas aeruginosa* and *Escherichia coli*, microorganisms. No zone of inhibition was observed for any of the ligands with 100 μL solution having a concentration of 1 $\mu\text{g}/\mu\text{L}$. MIC data denotes that all the ligands show poor antibacterial activity than complexes. All the complexes found more active against *S. marcescens*

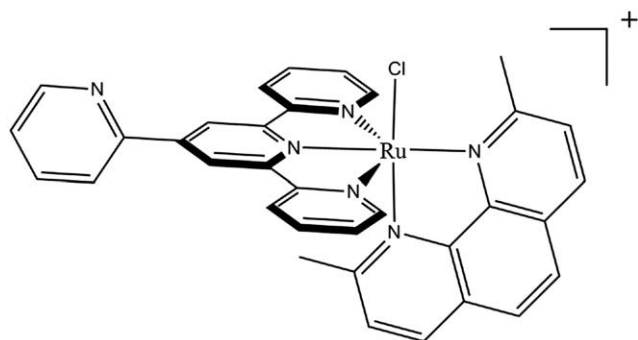


Fig. 1. Suggested structure of the complex $[Ru^{II}(2'''\text{-pytpy})(\text{dmphen})\text{Cl}](\text{ClO}_4)$ (**1**).

Table 1
Electronic spectral data for the ruthenium(II) complexes.

Complexes	$\lambda_{\text{max}}/\text{nm}$ ($\epsilon/\text{dm}^3\text{ mol}^{-1}\text{ cm}^{-1}$)		
	$\pi \rightarrow \pi^*$	MLCT	
$[Ru^{II}(2'''\text{-pytpy})(\text{dmphen})\text{Cl}](\text{ClO}_4)$ (1)	281 (45 714), 309 (46 190)	491 (18 670)	
$[Ru^{II}(3'''\text{-pytpy})(\text{dmphen})\text{Cl}](\text{ClO}_4)$ (2)	280 (46 545), 311 (42 356)	491 (18 750)	
$[Ru^{II}(3\text{-boptpy})(\text{dmphen})\text{Cl}](\text{ClO}_4)$ (3)	282 (56 386), 312 (52 740)	495 (21 340)	
$[Ru^{II}(4\text{-boptpy})(\text{dmphen})\text{Cl}](\text{ClO}_4)$ (4)	285 (57 283), 314 (56 132)	497 (22 210)	

and *E. coli* but found less active in the case of *P. aeruginosa*. All the complexes found less active than pefloxacin.

Binding of the compound with DNA through intercalation generally results in hypochromism and bathochromism due to the intercalative mode involving a strong stacking interaction of the planar aromatic chromophore of the compound with the base pairs of DNA [12]. Fig. 2 shows the absorption spectra of complex **1** in the presence of increasing amounts of DNA at room temperature. With increasing DNA concentration to complex **1**, hypochromism of the MLCT band at 493 nm was observed along with a 2 nm red shift. The red shift observed in complexes **2**, **3** and **4** is 2 nm, 1 nm and 1 nm, respectively. Similar red shift of the MLCT band reported for $[Ru(\text{phen})_2\text{NMP}]^{2+}$ and $[Ru(\text{tpy})(\text{PHNI})]^{2+}$ complexes [13,14]. So, small red shifting of the MLCT band suggests that the complexes may bind with DNA via partial intercalative mode.

In order to further investigate the binding strength of the complexes, the intrinsic binding constants (K_b) were determined by monitoring change in absorbance of the MLCT band with increasing concentration of DNA. The intrinsic binding constants (K_b) of complexes **1**, **2**, **3**, **4** were found to be 2.47×10^4 , 2.64×10^4 , 4.56×10^3 , $5.38 \times 10^3\text{ M}^{-1}$, respectively. The binding constants of ligands were found in the range of 1.35×10^3 to $4.43 \times 10^3\text{ M}^{-1}$, which are lower than intrinsic binding constants of the complexes. So, complexation increases the DNA binding affinity. The binding constants of complexes are smaller than that observed for $[Ru(\text{bpy})_2(\text{dppz})]$ ($>10^6$) [15]. The reason for the low binding constant is the presence of methyl groups on the 2nd and 9th positions of phenanthroline causing severe steric constraints near the Ru^{II} core when the complex intercalates to the DNA [16]. Another reason for low K_b is the nonplanarity of terpyridines.

Fig. 3 shows the plots of $[\text{DNA}]/(\epsilon_a - \epsilon_f)$ versus $[\text{DNA}]$ for $[Ru^{II}(2'''\text{-pytpy})(\text{dmphen})\text{Cl}](\text{ClO}_4)$ ($20\text{ }\mu\text{M}$) with increasing amount of DNA ($0\text{--}16.4\text{ }\mu\text{M}$) in phosphate buffer (pH 7.2), containing various concentrations of NaCl and incubated for 10 min at 37 °C. The non-

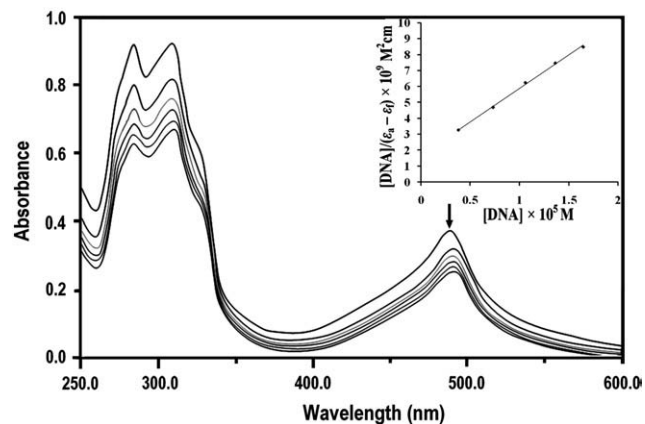


Fig. 2. Electronic absorption spectra of $[Ru^{II}(2'''\text{-pytpy})(\text{dmphen})\text{Cl}](\text{ClO}_4)$ with increasing amount of $[\text{DNA}]$ in phosphate buffer ($\text{Na}_2\text{HPO}_4/\text{NaH}_2\text{PO}_4$, pH 7.2), $[\text{complex}] = 20\text{ }\mu\text{M}$, $[\text{DNA}] = 0\text{--}16.4\text{ }\mu\text{M}$ with an incubation period of 10 min at 37 °C, inset: plot of $[\text{DNA}]/(\epsilon_a - \epsilon_f)$ versus $[\text{DNA}]$. Arrow shows the absorbance change upon increasing DNA concentrations.

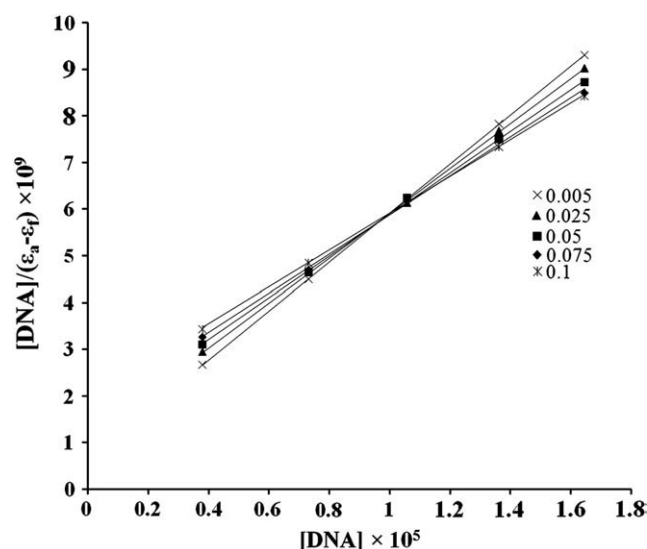


Fig. 3. Plots of $[DNA]/(\epsilon_a - \epsilon_f)$ versus $[DNA]$ for the spectrophotometric titration of $[Ru^{II}(2''\text{-pytpy})(\text{dmphen})\text{Cl}](\text{ClO}_4)$ with increasing amount of $[DNA]$ in phosphate buffer ($\text{Na}_2\text{HPO}_4/\text{NaH}_2\text{PO}_4$, pH 7.2) at 37°C and concentrations of NaCl varying from 0.005 to 0.1 M.

electrostatic binding constant (K_t^0) calculated using Eq. (1) and the data are summarized in Table 2.

$$\ln K_b = \ln K_t^0 + Z\xi^{-1}\{\ln(\gamma_{\pm}\delta)\} + Z\psi(\ln[M^+]) \quad (1)$$

where $Z\psi$ is the negative value of the slope obtained from the plots of $\log K_b$ versus $\log[M^+]$ (Fig. 4), ψ is the fraction of counter ions associated with each DNA phosphate ($\psi = 0.88$ for double-stranded B-form DNA), Z is the partial charge on the binding ligand, γ_{\pm} is the mean activity coefficient at cation concentration, where as remaining terms are constant for double-stranded B-form DNA, $\xi = 4.2$ and $\delta = 0.56$.

The magnitude of K_t^0 is constant throughout the experiment at various concentrations of NaCl with the average value of $8.593 \times 10^3 \text{ M}^{-1}$ (RSD limiting to 15%) but its contribution to K_b increases and reaches to 39.38% when the concentration of sodium ion reaches 0.1 M [17]. The salt concentration used during the course of study ranges from 0.001 to 0.1 M because the laws of theories of polyelectrolyte are only applicable if the concentration is higher than 0.1 M [18]. The value for the non-electrostatic DNA binding constant of synthesized complexes is about 36% at 0.075 M NaCl , which is higher compared to $[\text{Fe}(\text{phen})_2(\text{dppz})]^{2+}$ and classical intercalator ethidium bromide (EtBr) [19].

Dissection of binding free energy change (ΔG^0) during binding of complexes to DNA into electrostatic (ΔG_{pe}^0) and non-electrostatic (ΔG_t^0) free energy change at 0.075 M NaCl are summarized in Table 3 along with the data of $[\text{Fe}(\text{phen})_2(\text{dppz})]^{2+}$ [19]. The total binding

Table 2

Equilibrium binding constant (K_b) and contribution of the non-electrostatic binding constant (K_t^0) at various concentrations of NaCl .

$[\text{NaCl}]$ (M)	K_b (M^{-1}) ^a	K_t^0 (M^{-1}) ^b	K_t^0/K_b (%)
0.005	7.9159×10^4	8.059×10^3	10.18
0.025	4.4279×10^4	9.357×10^3	21.13
0.05	3.1399×10^4	9.049×10^3	28.82
0.075	2.4858×10^4	8.602×10^3	34.61
0.1	2.0059×10^4	7.900×10^3	39.38
Average K_t^0 (M^{-1}) = 8.593×10^3 ($\pm 0.624 \times 10^3$)			

^a K_b values are calculated as per Eq. (1).

^b K_t^0 values are calculated as per Eq. (2) with RSD less than 15%.

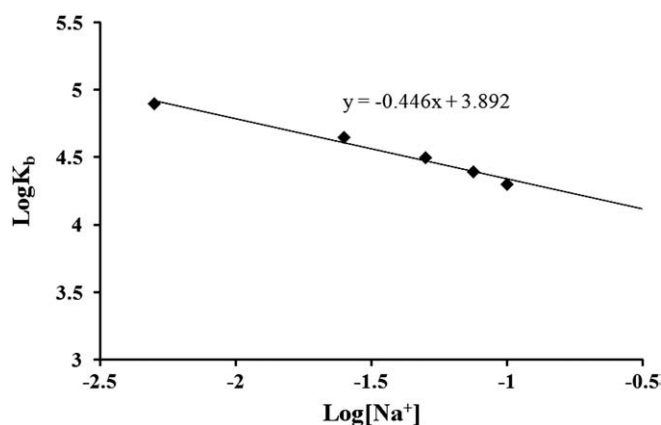


Fig. 4. Salt dependence of binding constant (K_b) for the binding of $[Ru^{II}(2''\text{-pytpy})(\text{dmphen})\text{Cl}](\text{ClO}_4)$ to DNA. The slope of this plot corresponds to the SK quantity presented in Table 3.

free energy changes (ΔG^0) were calculated based on the standard Gibbs relation (Eq. (2)). The data are represented in Table 3.

$$\Delta G^0 = -RT \ln K_b \quad (2)$$

where R is the gas constant and T is the absolute temperature.

The electrostatic free energy change (ΔG_{pe}^0) is calculated using Eq. (3) [20].

$$\Delta G_{pe}^0 = (SK)RT \ln [Na^+] \quad (3)$$

where salt dependence binding constant is defined as the slope of Fig. 4 (Eq. (4)).

$$SK = \delta \log K_b / \delta \log [Na^+] = -Z\psi \quad (4)$$

Non-electrostatic free energy change (ΔG_t^0) represents the binding free energy independent of salt concentration, which is defined as the difference of Gibbs free energy change ΔG^0 and electrostatic free energy change (ΔG_{pe}^0) and calculated using Eq. (5).

$$\Delta G_t^0 = \Delta G^0 - \Delta G_{pe}^0 \quad (5)$$

The melting of DNA is an important parameter to study the interaction of transition metal complexes with nucleic acids. Metal complexes bind to the double-stranded DNA, usually stabilize the duplex structure to some extent lead to an increase in the melting temperature (T_m) of DNA [21–23]. The melting temperature of DNA varies depending on the interacting strength of the compounds. The temperature at which 50% of the DNA has become single strand is known as melting temperature. It can be determined from the thermal denaturation curves of DNA by monitoring the absorption changes at 260 nm [24]. The T_m observed for DNA (100 μM) is $74.2 \pm 0.2^\circ\text{C}$ under our experimental conditions (Fig. 5).

In the presence of complexes **1**, **2**, **3**, **4**, the melting temperature (ΔT_m) of DNA increases by 4.7, 5.8, 2.7 and 2.9°C , respectively. These results show that the interaction of complex **2** with DNA is the strongest among all complexes.

In the absence of crystallographic study, hydrodynamic volume measurement is the most critical test to knock interaction properties [25]. A classical intercalation mode increases the viscosity of DNA solution by lengthening the DNA helix, while partial intercalation decreases the viscosity of DNA solution by reducing effective length of DNA [26]. The effect of the increasing amount of EtBr and complexes on the relative viscosity of DNA is shown in Fig. 6. EtBr is

Table 3

Thermodynamic parameters during the binding study of Herring Sperm DNA with complexes at 0.075 M concentration of NaCl.

Complex	$K_b/10^4 (M^{-1})$	ΔG^0	SK	ΔG_{pe}^0	$Kt^0/10^3 (Kt^0/K_b\%)$	$\Delta Gt^0 (\% \Delta Gt^0/\Delta G^0)$	Reference
1	2.4858	-25.07	0.440	-2.86	8.602 (34.61)	-22.21 (88.59)	This work
2	2.6544	-25.23	0.431	-2.76	9.519 (35.86)	-22.47 (89.04)	This work
3	0.4896	-21.05	0.422	-2.70	1.793 (36.64)	-18.34 (87.13)	This work
4	0.5672	-21.41	0.407	-2.61	2.153 (37.97)	-18.80 (87.80)	This work
[Fe(phen) ₂ (dppz)] ²⁺	9.5000	-28.39	0.493	-3.16	29.90 (31.46)	-25.23 (87.5)	[19]

a well known classical intercalator, which increases the relative viscosity of DNA solution. The decrease in relative viscosity of DNA solution by all ligands and complexes indicates that they interact with DNA via partial intercalation mode.

Fig. 7 shows the electrophoretic separation of pUC19 DNA upon reaction with complexes under aerobic condition. When the plasmid

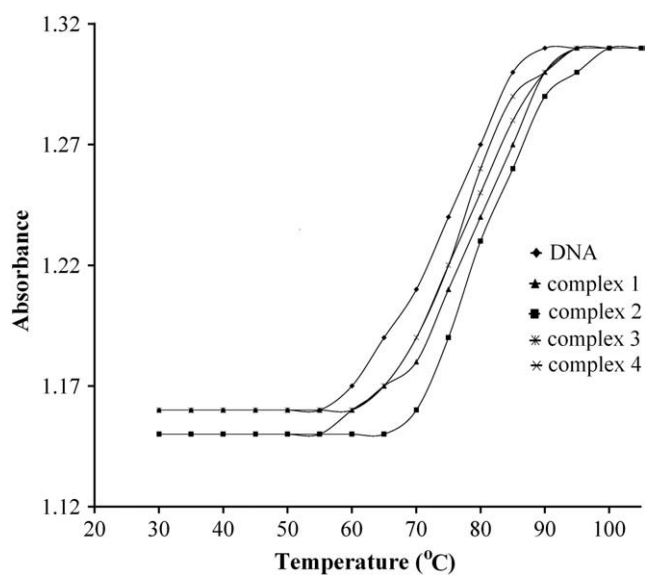


Fig. 5. Melting curves of DNA in the absence and the presence of the complexes **1, 2, 3, 4** ([DNA] = 100 μ M and [Complex] = 20 μ M, respectively).

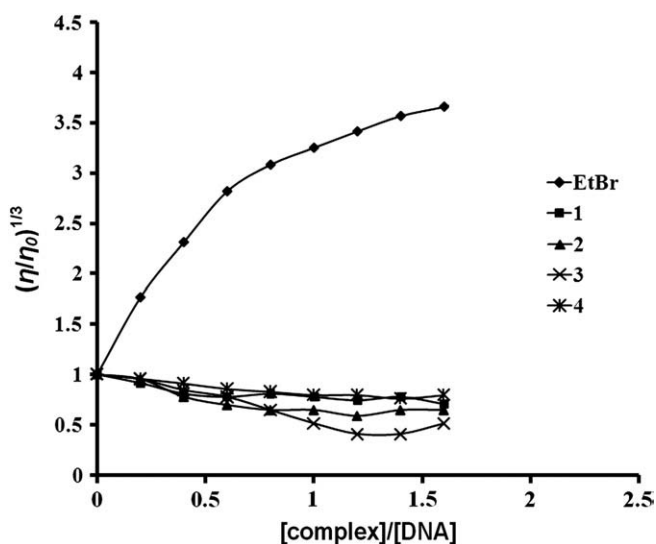


Fig. 6. Effect on the relative viscosity of DNA under the influence of increasing amount of ethidium bromide (EtBr) and complexes at 27 ± 0.1 °C in phosphate buffer ($\text{Na}_2\text{HPO}_4/\text{NaH}_2\text{PO}_4$, pH 7.2), as a medium.

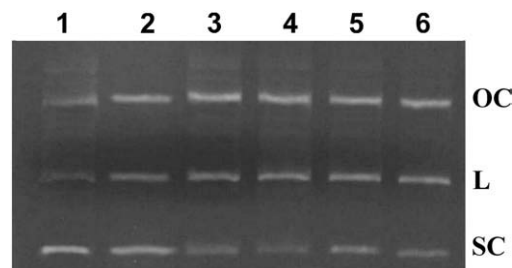


Fig. 7. Photograph of the interaction of pUC19 DNA (100 μ g/mL) with series of ruthenium(II) complexes (200 μ M) using 1% agarose gel containing 0.5 μ g/mL ethidium bromide (EtBr). All reactions were incubated in TE buffer (pH 8) in a final volume of 20 μ L, for 24 h at 37 °C: lane 1, DNA control; lane 2, RuCl_3 ; lane 3, $[\text{Ru}^{II}(2''\text{-pytpy})(\text{dmphen})\text{Cl}](\text{ClO}_4)$; lane 4, $[\text{Ru}^{II}(3''\text{-pytpy})(\text{dmphen})\text{Cl}](\text{ClO}_4)$; lane 5, $[\text{Ru}^{II}(3\text{-boptpy})(\text{dmphen})\text{Cl}](\text{ClO}_4)$; lane 6, $[\text{Ru}^{II}(4\text{-boptpy})(\text{dmphen})\text{Cl}](\text{ClO}_4)$.

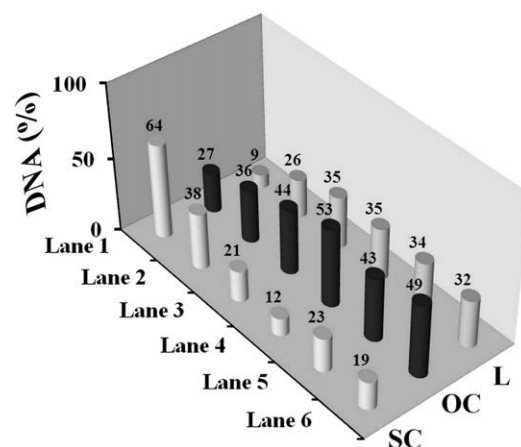


Fig. 8. Gel electrophoretic data of the DNA cleavage study.

DNA was subjected to electrophoresis upon reacting with complexes, the fastest migration was observed for super coiled (SC), the slowest moving open circular (OC) will produce upon relaxing of SC, the intermediate moving is the linear form (L) generated on the cleavage of the circular form. The data of the cleavage are presented in Fig. 8. From the data, it is clear that the complexes can cleave DNA more efficiently when compared to the metal salt. The difference in DNA cleavage efficiency of the complexes was due to the difference in binding affinity of the complexes to DNA.

Acknowledgements

Authors thank the head of the Department of Chemistry of Sardar Patel University, Vallabh Vidyanagar, India for making it convenient to work in the laboratory and U.G.C. for providing the financial support under "UGC Research Fellowship in Science for Meritorious Students" scheme.

Appendix A. Supplementary data

Supplementary data to this article can be found online at [doi:10.1016/j.inoche.2010.08.022](https://doi.org/10.1016/j.inoche.2010.08.022).

References

- [1] D.L. Arockiasamy, S. Radhika, R. Parthasarathi, B.U. Nair, *Eur. J. Med. Chem.* 44 (2009) 2044.
- [2] Y.J. Liu, H. Chao, J.H. Yao, L.F. Tan, Y.X. Yuan, L.N. Ji, *Inorg. Chim. Acta* 358 (2005) 1904.
- [3] L.S. Ling, Z.K. He, Y. Zeng, *Spectrochim. Acta A: Mol. Biomol. Spect.* 55 (1999) 1297.
- [4] G. Yang, J.Z. Wu, L. Wang, L.N. Ji, X. Tian, *J. Inorg. Biochem.* 66 (1997) 3807.
- [5] J.L. Morgan, D.P. Buck, A.G. Turley, J.G. Collins, F.R. Keene, *Inorg. Chim. Acta* 359 (2006) 888.
- [6] L.F. Tan, H. Chao, H. Li, Y.J. Liu, B. Sun, W. Wei, L.N. Ji, *J. Inorg. Biochem.* 99 (2005) 513.
- [7] Y.J. Liu, X.Y. Wei, F.H. Wu, W.J. Mei, L.X. He, *Spectrochim. Acta A: Mol. Biomol. Spect.* 70 (2008) 171.
- [8] C. Eva, A.C.G. Hotze, D.M. Tooke, A.L. Spek, J. Reedijk, *Inorg. Chim. Acta* 359 (2006) 830.
- [9] S. Goswami, A.R. Chakravarty, A. Chakravorty, *Inorg. Chem.* 21 (1982) 2737.
- [10] N. Yoshikawa, S. Yamabe, N. Kanehisa, Y. Kai, H. Takashima, K. Tsukahara, *Inorg. Chim. Acta* 359 (2006) 4585.
- [11] W. Henderson, J.S. McIndoe, *Mass Spectrometry of Inorganic, Coordination and Organometallic Compounds*, John Wiley & Sons Ltd, England, 2005.
- [12] S. Zhang, J. Zhou, *J. Coord. Chem.* 61 (2008) 2488.
- [13] C.-W. Jiang, H. Chao, H. Li, L.-N. Ji, *J. Inorg. Biochem.* 93 (2003) 247.
- [14] L.F. Tan, H. Chao, Y.J. Liu, H. Li, B. Sun, L.N. Ji, *Inorg. Chim. Acta* 358 (2005) 2191.
- [15] J.K. Barton, J.J. Dannenberg, A.L. Raphael, *J. Am. Chem. Soc.* 106 (1984) 2172.
- [16] Y.J. Liu, X.Y. Guan, X.Y. Wei, L.X. He, W.J. Mei, J.H. Yao, *Transition Met. Chem.* 33 (2008) 289.
- [17] T.C. Streckas, A.D. Baker, L. Zaltsman, S. Wang, *J. Coord. Chem.* 39 (1996) 281.
- [18] I. Haq, P. Lincoln, D. Suh, B. Norden, B.Z. Chowdhry, J.B. Chaires, *J. Am. Chem. Soc.* 117 (1995) 4788.
- [19] S. Mudasir, K. Wijaya, E.T. Wahyuni, N. Yoshioka, H. Inoue, *Biophys. Chem.* 121 (2006) 44.
- [20] S. Mudasir, K. Wijaya, N. Yoshioka, H. Inoue, *J. Inorg. Biochem.* 94 (2003) 263.
- [21] R. Rao, A.K. Patra, P.R. Chetana, *Polyhedron* 26 (2007) 5331.
- [22] R. Chen, C.-S. Liu, H. Zhang, Y. Guo, X.-H. Bu, M. Yang, *J. Inorg. Biochem.* 101 (2007) 412.
- [23] Y.-J. Liu, N. Wang, W.-J. Mei, F. Chen, L.-X. He, L.-Q. Jian, R.-J. Wang, *Transition Met. Chem.* 32 (2007) 332.
- [24] Y.-J. Liu, J.-C. Chen, F.-H. Wu, K.-C. Zheng, *Transition Met. Chem.* 34 (2009) 297.
- [25] X.W. Liu, J. Li, H. Li, K.C. Zheng, H. Chao, L.N. Ji, *J. Inorg. Biochem.* 99 (2005) 2372.
- [26] Y.J. Liu, J.F. He, J.H. Yao, W.J. Mei, F.H. Wu, L.X. He, *J. Coord. Chem.* 62 (2009) 665.